Phase-contrast microtomography with coherent high-energy synchrotron x rays

C. Raven,[a] A. Snigirev, I. Snigireva, P. Spanne, A. Souvorov, and V. Kohn[b]
ESRF, B.P. 220, F-38043 Grenoble Cedex, France

(Received 1 April 1996; accepted for publication 11 July 1996)

Cross-sectional information on low electron density materials can be obtained by probing a sample with a 60 keV coherent synchrotron x-ray beam in an in-line holography setup. Such objects are practically transparent to high energy x rays and create a phase shift of the wave front only. Images of a 100 μm diameter boron fiber were recorded in the extreme near field region, where contrast occurs only at interfaces between regions with different decrements of refractive index. Theoretical simulations are in good agreement with the measured intensities. In a tomographic reconstruction the 15 μm diameter core of the fiber is clearly visible, demonstrating the possibility of reconstructing three dimensional interfaces between low density materials. © *1996 American Institute of Physics.* [S0003-6951(96)01939-0]

Probing organic samples and low electronic density materials with high energy x rays has advantages over soft x rays because thicker samples can be investigated with lower absorbed dose. However, there is almost no absorption contrast, since the absorption index β, i.e., the imaginary part of the refractive index $n=1-\delta+i\beta$, is very close to unity for high energy x rays and varies only slightly with the atomic number Z.[1] More sensitive measurements can be obtained from the decrement δ of the refractive index by measuring the phase of the wave field. Since the phase cannot be measured directly, several indirect methods have been reported. For soft x rays, holography[2,3] and phase-contrast microscopy with zone plates in a Zernicke-type setup[4] have been used. For hard x rays two-beam interferometry[5,6] and analyzer crystals[7] have been employed. Recently, high-energy phase-contrast imaging with an in-line holography setup using the coherence properties of a third generation synchrotron x-ray source was presented.[8,9] However, in some applications quantitative mapping of the refractive index is not necessary and a type of qualitative imaging revealing boundaries between different components in a sample is sufficient. Such imaging can be performed by combining a holography setup using the coherence properties of third generation synchrotron radiation sources and a computed tomography reconstruction algorithm.

Consider a carthesian coordinate system with z parallel to the beam direction and an elongated sample with a refractive index gradient along the x-axis only, i.e., a cylindrical fiber (Fig. 1). With such a sample the radiation field in the detector plane can be written as[8]

$$E(x,y)=E_0(x,y)[1+c(x)], \tag{1}$$

where $E_0$is the incident wave and $c(x)$ is a contrast function given by

$$c(x)=\frac{1}{\sqrt{i\lambda r}}\int_{-d/2}^{d/2}\exp\left(\frac{2\pi i}{\lambda}\frac{(x-\tilde{x})^2}{2r}\right)\{\exp[i\theta(\tilde{x})]-1\}d\tilde{x}, \tag{2}$$

with the total phase shift along the beam

$$\theta(\tilde{x})=\frac{2\pi}{\lambda}\int_{-d/2}^{d/2}\delta(\tilde{x},z)dz. \tag{3}$$

Here λ is the wavelength of the incident beam, r the distance from the sample to the detector plane, and d the diameter of the sample. Equation (2) is valid for a coherent beam from a point source. For a finite source size, this expression has to be convolved with the source distribution to give the contrast function. The term $\exp[2\pi i(x-\tilde{x})^2/2\lambda r]$ in the integral in Eq. (2) represents the propagation of the wave from the sample to the detector,[10] the second term $\{\exp[i\theta(\tilde{x})]-1\}$ is due to the phase shift in the sample. To obtain significant contrast, $\theta(\tilde{x})$ must change considerably within a distance $\xi=x-\tilde{x}$ given by $\xi<\sqrt{\lambda r}$. In our experiment with $r=2$ m and $\lambda=0.21$ Å, ξ was about $6\,\mu$m. Thus the holograms show phase contrast exclusively at interfaces parallel to the beam direction because only there does $\theta(\tilde{x})$ change significantly within a distance ξ.

In absorption tomography, the logarithm of the number of photons entering the object, N_{in}, over the number of photons leaving the sample, N_d

$$\ln\frac{N_{in}}{N_d}=\int_{\text{ray}}\mu(x,z)ds=\frac{4\pi}{\lambda}\int_{\text{ray}}\beta(x,z)ds, \tag{4}$$

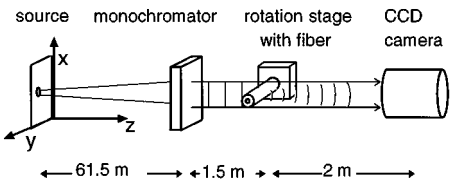

FIG. 1. Schematic setup of the experiment. A phase-contrast image is recorded in an in-line holographic geometry.

[a]Electronic mail: raven@esrf.fr
[b]Permanent address: Russian Research Centre ''Kurchatov Institute,'' 123182 Moscow, Russia.

 0003-6951/96/69(13)/1826/3/$10.00

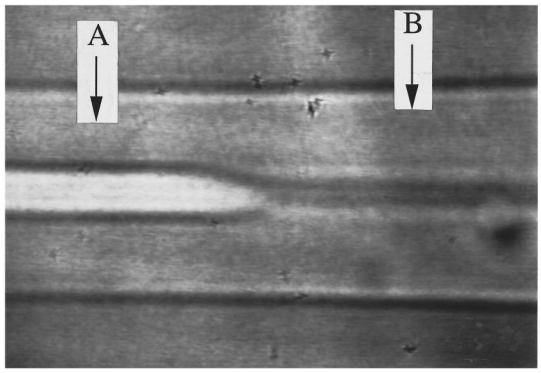

FIG. 2. X-ray image of the fiber at 2 m distance on high resolution film. The fiber edges are seen as well as the tungsten core on the left-hand side and the remaining hollow core after etching on the right-hand side. Lines A and B show the positions where the intensity distribution of Fig. 3 were taken.

is used to reconstruct the distribution of the linear attenuation coefficient μ, or the absorption index β, of the material in the tomographic slice.[11] The contrast function $c(x)$, which arises from the propagation of the phase modulated wave front from the object to the detector, can formally be regarded as a modulation of the incoming wave due to an absorptionlike function $b(x,z)$

$$|1+c(x)|^2=\exp\int b(x,z)dz. \tag{5}$$

The absorptionlike function $b(x,z)$ is different from zero only where $c(x)$ shows significant values, thus only at interfaces parallel to the beam direction. We obtain $b(x,z)$ for all x and z from different views by rotating the sample. The nonzero values of $b(x,z)$ indicate the interfaces in the sample.

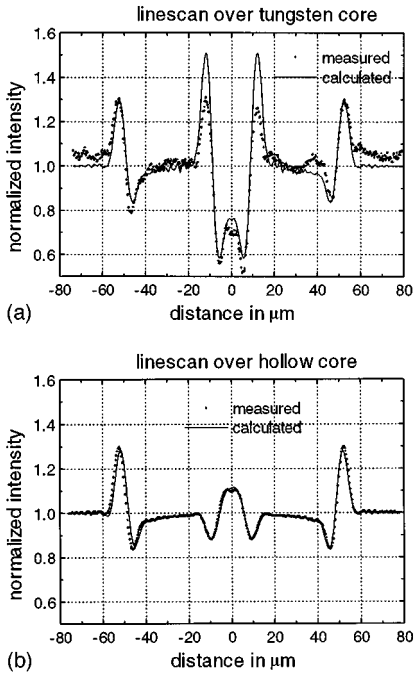

FIG. 3. Intensity distribution across the fiber of Fig. 2: (a) with tungsten core, (b) over hollow core. The intensities are normalized to the homogeneous background intensity without the fiber.

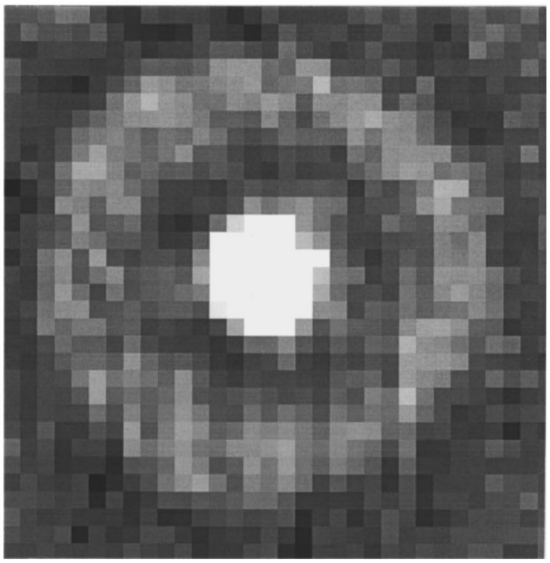
(a)

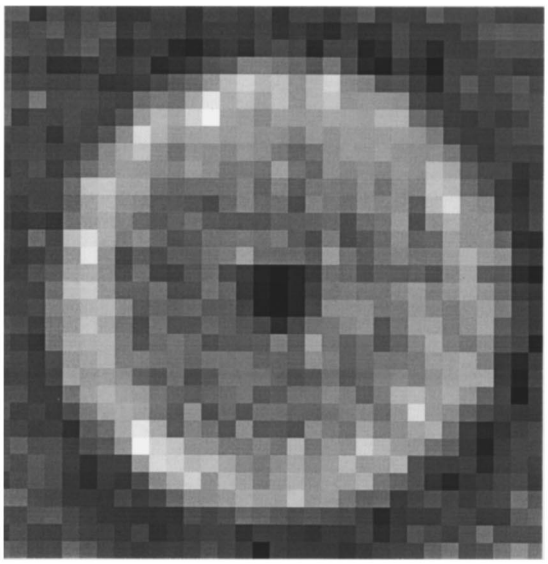
(b)

FIG. 4. Reconstructed tomographic cross sections: (a) with tungsten core, (b) with hollow core. The tungsten core appears larger than the hollow core due to lens effects.

The experiment was done at the ESRF high-energy wiggler beamline ID 15. It delivers an x-ray beam with 0.14 $\times$0.1 mm^2 source size and a divergence of 0.18$\times$ 0.03 mrad^2. The beam was monochromatized to 60 keV ($\lambda=0.21$ Å) using the 531 reflection of a Si monochromator in Laue geometry. Figure 1 shows a schematic view of the experimental setup. The sample was mounted on a horizontal rotation stage to take advantage of the fact that the spatial coherence is higher in vertical than in the horizontal direction due to the rectangular source size.

As an object a 100 μm diameter boron fiber with a 15 μm tungsten core was used. From one end of the fiber, the core had been etched electrochemically. Phase-contrast images of the boron fiber were recorded on high resolution film at a sample-to-film distances of 2 m. The outside edges of the fiber and the boundary to the inner core are clearly seen (Fig. 2). The intensity distributions across the fiber over the

tungsten core and over the hollow core are shown in Fig. 3. Measured and calculated intensities show contrast up to 30%–40% at the interfaces. For the tomographic reconstruction we recorded 61 two-dimensional projections over 180° using a high resolution, cooled CCD-based x-ray detector with a dynamical range of 8 bits. A fiber optic system projects the light from an 8-μm-thick gadolinium oxysulfide scintillator onto the CCD. The exposure time for each image was about 25 s. The tomographic reconstruction was performed using a filtered backprojection algorithm. In both tomograms of Fig. 4 the outer surface of the boron fiber is visible as well as the core. The tungsten core appears significantly larger due to the high absorption and to lens effects introduced by the different refractive indices. For x rays tungsten has a smaller refractive index than boron and the core acts like a defocusing lens. Air, on the other side, has a higher refractive index than the surrounding boron fiber for x rays and the hollow core can thus be regarded as a focusing lens. Note that the reconstructed values do not correspond to the refractive index over the fiber but rather emphasize the regions with an abrupt change in the refractive index, thus indicating interfaces and borders in the sample.

The results demonstrate the feasibility of phase-contrast tomography using the coherence properties of a third generation synchrotron x-ray source. The large distance between sample and detector offers easy access to the sample and the possibility of installing large sample chambers such as high-pressure cells or cryostats. On the other hand, it must be recognized that the reconstruction method used here is only approximate. A reconstruction algorithm for accurate quantization of the refractive index has to take into account the intrinsic image formation process. The drawback in this experiment is the limited resolution of the CCD system, where CCD pixel size, the grain size of the polycrystalline scintillator, and the fiber optics sum up to a spatial resolution of 10 μm. Nevertheless, a qualitative reconstruction technique and a resolution in three dimensions of about 10 μm is sufficient to begin many material and biological studies.

We wish to thank J.-M. Rigal for technical support during the experiment and M. Kocsis for providing the boron fiber sample. We also acknowledge the assistance of T. Tschentscher, P. Suortti, K.-D. Liss, and U. Kleuker during the experiment at the high-energy beamline.

[1] G. Schmahl, D. Rudolph, and P. Guttmann, in *X-Ray Microscopy II*, edited by D. Sayre, M. Howells, J. Kirz, and H. Rarback (Springer, Berlin, 1988), pp. 228–232.
[2] I. McNulty, J. Kirz, C. Jacobsen, E. H. Anderson, M. R. Howells, and D. P. Kern, Science **256**, 1009 (1992).
[3] M. R. Howells, C. J. Jacobsen, and S. Lindaas, in *X-Ray Microscopy IV*, edited by V. V. Aristov and A. I. Erko (Bogorodskii Pechatnik, Chernogolovka, 1994), pp. 414–428.
[4] G. Schmahl, P. Guttmann, G. Schneider, B. Niemann, C. David, T. Wilhein, J. Thieme, and D. Rudolph, in *X-Ray Microscopy IV*, edited by V. V. Aristov and A. I. Erko (Bogorodskii Pechatnick, Chernogolovka, 1994), pp. 196–206; B Niemann, G. Schneider, P. Guttmann, D. Rudolph, and G. Schmahl, *ibid*., pp. 66–75.
[5] U. Bonse and M. Hart, Appl. Phys. Lett. **6**, 155 (1965).
[6] A. Momose, T. Takeda, Y. Itai, and K. Hirano, Nat. Med. **2**, 473 (1996).
[7] V. N. Ingal and E. A. Beliaevskaya, J. Phys. D **28**, 2314 (1995).
[8] A. Snigirev, I. Snigireva, V. Kohn, S. Kuznesov, and I. Schelokov, Rev. Sci. Instrum. **66**, 5486 (1995).
[9] A. Snigirev, I. Snigireva, V. Kohn, and S. Kuznetsov, Nucl. Instrum. Methods Phys. Res. A **370**, 634 (1996).
[10] J. M. Cowley, *Diffraction Physics* (North-Holland, Amsterdam, 1990).
[11] A. C. Kak and M. Slaney, *Principles of Computerized Tomographic Imaging* (IEEE, New York, 1988).